

Evaluated $^{238}\text{U}(\text{n},\text{f})$ Average Prompt Fission Neutron Multiplicities Including the CGMF Model

D. Neudecker, A.E. Lovell, T. Kawano, P. Talou
Los Alamos National Laboratory, Los Alamos, NM, 87545, USA

September 28, 2022

5 Contents

6	1	Introduction	2
7	2	Evaluation Input and Algorithms	2
8	2.1	Model Input	2
9	2.2	Experimental Input	3
10	2.3	Evaluation Methods	5
11	3	Results	6
12	3.1	Evaluated Results of $^{238}\text{U}(\text{n},\text{f}) \bar{\nu}_p$ Based on Only Experimental Data	6
13	3.2	Evaluated Results of $^{238}\text{U}(\text{n},\text{f}) \bar{\nu}_p$ Including CGMF	7
14	3.3	Validation of Evaluated Parameters Against Various Fission Data	7
15	4	Conclusions and Outlook	11
16	5	Point of contact	13
17	A	Comments on Experimental Data for $^{238}\text{U} \bar{\nu}_p$	15

Abstract

This report documents an evaluation of the average prompt fission neutron multiplicity, $\bar{\nu}_p$, of ^{238}U from 800 keV to 20 MeV. This evaluation had to be re-done from “scratch” as the input to previous $\bar{\nu}_p$ evaluations, specifically ENDF/B-VIII.0, was not found. That means that all available experimental data were re-analyzed and uncertainties were re-estimated. The new evaluated ^{238}U $\bar{\nu}_p$ based on only experimental data differs distinctly from ENDF/B-VIII.0 $\bar{\nu}_p$ from 2 to 4.5 MeV, and from 6 to 7 MeV, and is otherwise similar. The difference from 2 to 4.5 MeV stems from the fact that ENDF/B-VIII.0 was tweaked in this energy range to data of Frehaut, while two other, equally trustworthy, data sets would indicate an evaluated ^{238}U $\bar{\nu}_p$ that is up to 2% higher. Also, second chance fission in ENDF/B-VIII.0 was smoothed over from 6–7 MeV. Another major difference to ENDF/B-VIII.0 is that one of the evaluations presented here includes model information from the Hauser-Feshbach fission fragment decay code CGMF, while ENDF/B-VIII.0 is based purely on experimental data. CGMF links several fission quantities with each other; $\bar{\nu}_p$ is predicted by assumptions made on, e.g., pre-neutron emission yields as a function of mass, the total kinetic energy, or spin and parity of fission fragments. This allows to validate the new ^{238}U $\bar{\nu}_p$ by using CGMF parameters obtained from fitting to experimental ^{238}U $\bar{\nu}_p$ to predict yields as a function of mass, the average total kinetic energy, or the mean energy of the prompt fission neutron spectrum. These model-predicted values can then be compared to experimental and evaluated data. The model-predicted fission-observable values using evaluated parameters obtained here are reasonably close to experimental data for some observables, but are farther away from experimental data related

38 to TKE observables. In addition to that, the evaluated $^{238}\text{U}(\text{n,f}) \bar{\nu}_p$ shows similar deviations from
39 ENDF/B-VIII.0 as for the evaluation with only experimental data. This difference is expected
40 to lead to changes in simulated effective neutron multiplication factor, k_{eff} of ICSBEP critical
41 assemblies that are sensitive to ^{238}U in the fast range (BigTen, Flattop, Flattop-Pu). These changes
42 in k_{eff} need to be counter-balanced. Chi-Nu PFNS experimental data are expected to be released
43 in the next few months that might lead to the needed changes in the PFNS. Until then, we hold
44 off in benchmarking the new $^{238}\text{U}(\text{n,f}) \bar{\nu}_p$ as well as submitting it to ENDF/B-VIII.1. Also, new
45 high-precision $^{238}\text{U} \bar{\nu}_p$ are expected to be measured by the CEA in the next two years that will
46 shed further light on question on $^{238}\text{U} \bar{\nu}_p$ from 2–4.5 and 6–7 MeV.

47 **Keywords:** ^{238}U , Average Prompt Fission Neutron Multiplicity, CGMF.

48 LA-UR-22-29906

49 1 Introduction

50 This report documents our progress towards an FY22 NCSP (Nuclear Criticality Safety Program) mile-
51 stones for LANL: “ ^{238}U : Evaluate PFNS and multiplicity consistently, including angular information
52 about prompt neutrons”. In this report, we show that we evaluated $^{238}\text{U}(\text{n,f}) \bar{\nu}_p$ (termed “multiplicity”
53 in the milestone text) with the code CGMF [1]. CGMF provides concurrently $\bar{\nu}_p$, angular information and
54 prompt fission neutron spectra (PFNS), and thus satisfies the milestone.

55 Previously, progress on and final evaluations of ^{235}U and $^{239}\text{Pu} \bar{\nu}_p$ have been documented in Refs. [2–
56 4]. This report builds upon all of them and uses text of Refs. [2,3] where the same input or procedures
57 were applied.

58 In order to undertake this evaluation, we started with a detailed uncertainty estimate and analysis
59 of all experimental data, as described in Section 2.2. This provided evaluated $^{238}\text{U}(\text{n,f}) \bar{\nu}_p$ based on
60 only experimental data discussed in Section 3.1. On top of this, the CGMF model (Section 2.1) was added
61 by the Kalman filter technique described in Section 2.3. The evaluated data shown in Section 3.2 is
62 similar to the evaluation based on only experimental data, except for second-chance fission, showing the
63 CGMF is for most energies able to correctly evaluate $^{238}\text{U}(\text{n,f}) \bar{\nu}_p$. Also, the evaluated parameters fitted
64 to $^{238}\text{U}(\text{n,f}) \bar{\nu}_p$ were forward-propagated via CGMF to predict various post-scission fission observables
65 shown in Section 3.3, and are close to experimental data for many observables but not to experimental
66 data related to TKE observables. Given the close agreement of evaluated $^{238}\text{U}(\text{n,f}) \bar{\nu}_p$ with and without
67 CGMF, and reliable prediction of some post-scission fission quantities, it makes the evaluated $^{238}\text{U}(\text{n,f})$
68 $\bar{\nu}_p$ based on CGMF in principle eligible to be proposed as a release candidate for an evaluation project.

69 However, the new evaluated $^{238}\text{U}(\text{n,f}) \bar{\nu}_p$, with and without CGMF, differ distinctly from ENDF/B-
70 VIII.0 for 2 to 4.5 MeV due to a tweak in the latter data. This will change the effective neutron
71 multiplication factor of ICSBEP critical assemblies sensitive to $^{238}\text{U}(\text{n,f}) \bar{\nu}_p$ in the fast range. We need
72 to counter-balance that, and will thus wait for an upcoming evaluation of the ^{238}U PFNS, that will be
73 informed by upcoming Chi-Nu data, before introducing the new $^{238}\text{U}(\text{n,f}) \bar{\nu}_p$ into a release candidate
74 file. Alsp, new $^{238}\text{U} \bar{\nu}_p$ will be measured by CEA that will further inform us on the $\bar{\nu}_p$ from 2–4.5
75 and 6–7 MeV. Until then, we recommend to hold off on including the new evaluated in the ENDF/B
76 library.

77 2 Evaluation Input and Algorithms

78 2.1 Model Input

79 To consistently evaluate multiple prompt fission observables, we use the LANL-developed Hauser-
80 Feshbach fission fragment decay code, CGMF [1]. CGMF takes input for the fission fragment initial
81 conditions—yields in mass, charge, total kinetic energy, spin, and parity—which are sampled on an

82 event-by-event basis. Starting from these initial conditions, the fission fragments are allowed to de-
 83 excite through the emission of neutrons and γ rays. At high enough incident energies, where one
 84 or more neutrons can be emitted before the compound nucleus fissions, we sample the multi-chance
 85 fission probabilities (calculated from CoH) based on whether neutrons are emitted from the compound
 86 nucleus before fission; we also sample properties of these neutrons. All of the steps in the CGMF
 87 calculation require inputs not only for the fission fragment initial conditions, but also many global
 88 models that are used in the Hauser-Feshbach decay. However, for this evaluation work, we only vary the
 89 parameters in the pre-neutron emission mass yields, $Y(A|E_{\text{inc}})$, total kinetic energy parameterizations,
 90 $\text{TKE}(E_{\text{inc}})$, $\text{TKE}(A)$, and $\sigma_{\text{TKE}}(A)$, and the spin cutoff factor in the spin distribution, $\alpha(E_{\text{inc}})$. A
 91 detailed description of these parameters are found in our NCSP report from FY20 [4] along with the
 92 published version of the CGMF code [1].

93 2.2 Experimental Input

94 All ^{238}U $\bar{\nu}_p$ experimental data listed in Table I were extracted from EXFOR. The EXFOR entry and,
 95 if available, the literature of each data set was studied in enough detail to decide whether it should
 96 be adopted or not. One data set was rejected because it provided data above the energy range of the
 97 evaluation. Other data sets were rejected for physics reasons, or because of inadequate uncertainty
 98 information on the data set. The reasons for rejecting individual ^{238}U $\bar{\nu}_p$ experimental data sets are
 99 briefly summarized in Appendix A.

Table I: Those $^{238}\text{U}(\text{n,f})$ $\bar{\nu}_p$ experimental data sets included in the evaluation are identified with their EXFOR No., first author, year of publication, monitor, and E_{inc} range. The last column tabulates all uncertainty sources that were added to those uncertainties found in the literature of the respective data set. The variable names are defined in Table II.

EXFOR #	First Author & Year	Monitor	E_{inc} (MeV)	Added Unc.
20075.002	Asplund 1964 [5]	$^{252}\text{Cf(sf)}$ $\bar{\nu}_p$	1.49–14.8	$\delta c_{DG}, \delta b, \delta c_{ff}, \delta \omega, \delta \chi, \delta a, \delta d, \delta d_{s/m}$
20072.003	Conde 1961 [6]	$^{252}\text{Cf(sf)}$ $\bar{\nu}_p$	3.6–14.9	$\delta c_{DG}, \delta b, \delta c_{ff}, \delta \omega, \delta \chi, \delta a, \delta d, \delta d_{s/m}$
33084.003	Desai 2015 [7]	$^{252}\text{Cf(sf)}$ $\bar{\nu}_p$	2–3	$\delta b, \delta \omega, \delta \tau, \delta a, \delta d, \delta d_{s/m}$
21252.004	Fieldhouse 1966 [8]	$^{252}\text{Cf(sf)}$ $\bar{\nu}_p$	14.2	$\delta c_{DG}, \delta b, \delta c_{ff}, \delta \omega, \delta \tau, \delta \chi, \delta a, \delta d$
20490.002	Frehaut 1980 [9]	$^{252}\text{Cf(sf)}$ $\bar{\nu}_p$	1.36–14.79	$\delta c_{DG}, \delta b, \delta c_{ff}, \delta \omega, \delta \tau, \delta \chi, \delta a, \delta d$
21453.002	Leroy 1960 [10]	$^{235}\text{U}(\text{n,f})$ $\bar{\nu}_p$	14.2	$\delta c_{DG}, \delta b, \delta c_{ff}, \delta \omega, \delta \tau, \delta a, \delta d, \delta d_{s/m}$
21135.006	Mather 1965 [11]	$^{252}\text{Cf(sf)}$ $\bar{\nu}_t$	1.4–4.02	$\delta c_{DG}, \delta b, \delta \tau, \delta a, \delta d, \delta d_{s/m}$
40429.003	Nurpeisov 1975 [12]	$^{252}\text{Cf(sf)}$ $\bar{\nu}_t$	1.2–4.89	$\delta c_{DG}, \delta \omega, \delta d_{s/m}$
40138.002	Sabin 1972 [13]	$^{252}\text{Cf(sf)}$ $\bar{\nu}_p$	1.27–5.87	$\delta c_{DG}, \delta c_{ff}, \delta \omega, \delta \tau, \delta a, \delta d, \delta d_{s/m}$
40665.002	Vorobyeva 1981 [14]	$^{252}\text{Cf(sf)}$ $\bar{\nu}_p$	1.3–5.89	$\delta c_{DG}, \delta c_{ff}, \delta \omega, \delta \tau, \delta a$
32606.002	Zangyou 1975 [15]	$^{240}\text{Pu(sf)}$ $\bar{\nu}_t$	1.22–5.5	$\delta c_{DG}, \delta b, \delta c_{ff}, \delta \omega, \delta a, \delta d, \delta d_{s/m}$

100 A detailed uncertainty estimate and literature review was undertaken for all data sets in Table II.

Table II: Typical uncertainty sources expected to apply to ratio liquid-scintillator measurements of $\bar{\nu}_p$ are listed. The variable names defined in this table are used for the last column of Table I.

Variable	Uncertainty Source
δc_{DG}	Delayed Gamma-ray Uncertainties
δb	Random-background Uncertainties
δc_{ff}	False-fission Uncertainties
$\delta \omega$	Impurity Uncertainties
$\delta \tau$	Deadtime Uncertainties
$\delta \chi$	PFNS Uncertainties
δa	Uncertainties of Angular Distribution of Fission Neutrons
$\delta \bar{\nu}^m$	Monitor Uncertainties
δd	Uncertainty due to Thickness of Sample
$\delta d_{s/m}$	Sample-displacement Uncertainty
ΔE_{inc}	Energy Uncertainty

101 Appendix A concisely summarizes some key concerns on each data set and comments on the individual
 102 uncertainty estimate.

The uncertainty was undertaken via the code package ARIADNE [16]. Consistent uncertainty values for those that were missing in the literature or EXFOR or both were estimated via templates of expected uncertainties for ratio $\bar{\nu}$ measurements [17] accounting for uncertainty sources listed in Table II. Total experimental covariances, $\text{Cov}_{i,j}^{tot}$, were estimated by

$$\text{Cov}_{i,j}^{tot} = \sum_k \delta_i^k \text{Cor}_{i,j}^k \delta_j^k, \quad (1)$$

103 accounting for individual uncertainty values, δ_i^k , and correlation coefficients, $\text{Cor}_{i,j}^k$, for each expected
 104 uncertainty source k at incident-neutron energy i or j . The monitor uncertainty was a major one
 105 for most measurements contributing 0.42% with full correlation. This uncertainty was applied across
 106 all data sets to account for uncertainties in the current $^{252}\text{Cf(sf)}$ $\bar{\nu}$ put forth by the Neutron Data
 107 Standards committee [18]. While not all data were measured in ratio to this particular reaction, all of
 108 them were ratio measurements that tie back to a monitor reaction that either relies itself on $^{252}\text{Cf(sf)}$
 109 $\bar{\nu}$ if it isn't $^{252}\text{Cf(sf)}$ $\bar{\nu}$ to begin with.

110 In addition to the experimental data listed in Table I, evaluated data were used as “pseudo-
 111 experimental” data. These pseudo-experimental data are listed in Table III. They are given as anchor
 112 points for the evaluation from 0.8–1.12 and greater equal 15 MeV, where experimental data are scarce.

Table III: Pseudo-experimental data as used for the $\bar{\nu}_p$ evaluation are listed as a function of energy and along with their uncertainties. All pseudo-experimental data were taken from ENDF/B-VIII.0 [19].

Energy (MeV)	Value (n/f)	Unc. (%)
0.8	2.4689	1.2
0.84	2.4726	1.2
0.96	2.4836	1.2
1.0	2.4862	1.2
1.12	2.4973	1.2
15.0	4.573	1.2
16.0	4.72	1.2
30.0	6.388	1.2

2.3 Evaluation Methods

This part is a shortened repeat from Ref. [3] as the same evaluation techniques were used. We use two evaluation techniques implemented in the code ARIADNE [16]:

- generalized least squares for evaluations including only experimental data, and
- the Kalman filter method to combine information from CGMF and experimental data.

Both can be encoded in the same set of equations, that give a vector of evaluated mean values \mathbf{N} and Cov^N ,

$$\begin{aligned}\mathbf{N} &= \mathbf{p} + \text{Cov}^N \mathbf{S}^t (\text{Cov}^{e,i})^{-1} (\mathbf{e} - \mathbf{S}\mathbf{p}), \\ \text{Cov}^N &= \text{Cov}^p - \text{Cov}^p \mathbf{S}^t Q^{-1} \mathbf{S} \text{Cov}^p,\end{aligned}\quad (2)$$

where

$$Q = \mathbf{S} \text{Cov}^p \mathbf{S}^t + \text{Cov}^e. \quad (3)$$

The variables \mathbf{e} and $\text{Cov}^{e,i}$ encode all experimental data used for the evaluation and their covariances estimated as described in Section 2.2.

If we apply the equations above in the sense of **generalized least squares** (GLS), \mathbf{p} and Cov^p contain non-informative prior information in the $\bar{\nu}_p$ space, *i.e.*, ENDF/B-VIII.0 mean values with 100% uncertainty and a diagonal covariance matrix. The design matrix \mathbf{S} and its transpose \mathbf{S}^t were calculated in Ref. [20] by linear interpolation to bring experimental data onto the E_{inc} grid of the prior data. The evaluated mean values \mathbf{N} and Cov^N correspond in this case to evaluated $\bar{\nu}_p$ and their covariances.

If we apply Eq. (2) as a **Kalman filter**, \mathbf{p} turns into model-parameter values and Cov^p into associated covariances. The design matrix converts experimental data into model-parameter space by taking sensitivity vectors as described in Ref. [2]. The evaluated mean values \mathbf{N} and Cov^N correspond in this case to evaluated model parameters of CGMF that are then fed again into the model code to obtain an evaluated $\bar{\nu}_p$.

It should be noted that the experimental covariances were corrected for an effect termed “Peelle’s Pertinent Puzzle” [22] using the Chiba-Smith algorithm [23]. Peelle’s Pertinent Puzzle is an effect where the evaluated mean value of strongly correlated experimental data lies outside of the range of the experimental data due to an improperly formulated covariance matrix [21]. Chiba-Smith is a special case of iterative generalized least squares where the experimental covariance matrix in Eq. (2) is changed in the first iteration to:

$$\text{Cov}_{jk}^{e,1} = \text{Cov}_{jk}^{e,0} \frac{m_j^0 m_k^0}{e_j e_k}, \quad (4)$$

where m_j^0 and m_k^0 are prior model values of $\bar{\nu}_p$ on the grid of the experimental values j and k , while e_j and e_k are the experimental values. $\text{Cov}_{jk}^{e,0}$ are the experimental covariances as coming out of ARIADNE [16]. For subsequent iterations, $i > 1$:

$$\text{Cov}_{jk}^{e,i+1} = \text{Cov}_{jk}^{e,i} \frac{m_j^{i+1} m_k^{i+1}}{m_j^i m_k^i}, \quad (5)$$

where \mathbf{m}^i are evaluated mean values of $\bar{\nu}_p$ of iteration i on the grid of experimental data to give m^i . For the Kalman filter \mathbf{m}^i is obtained by first obtaining the evaluated $\bar{\nu}^i$ of iteration i :

$$\bar{\nu}_p^i = \bar{\nu}_p^0 + \mathbf{S}(\mathbf{N}^i - \mathbf{p}), \quad (6)$$

where $\bar{\nu}_p^0$ are prior mean values on the original grid of model $\bar{\nu}_p$ values. The $\bar{\nu}_p^i$ values are then linearly interpolated onto the grid of experimental data to yield \mathbf{m}^i . For generalized least square, \mathbf{m}^i is obtained by linearly interpolating \mathbf{N}^i onto the grid of experimental data.

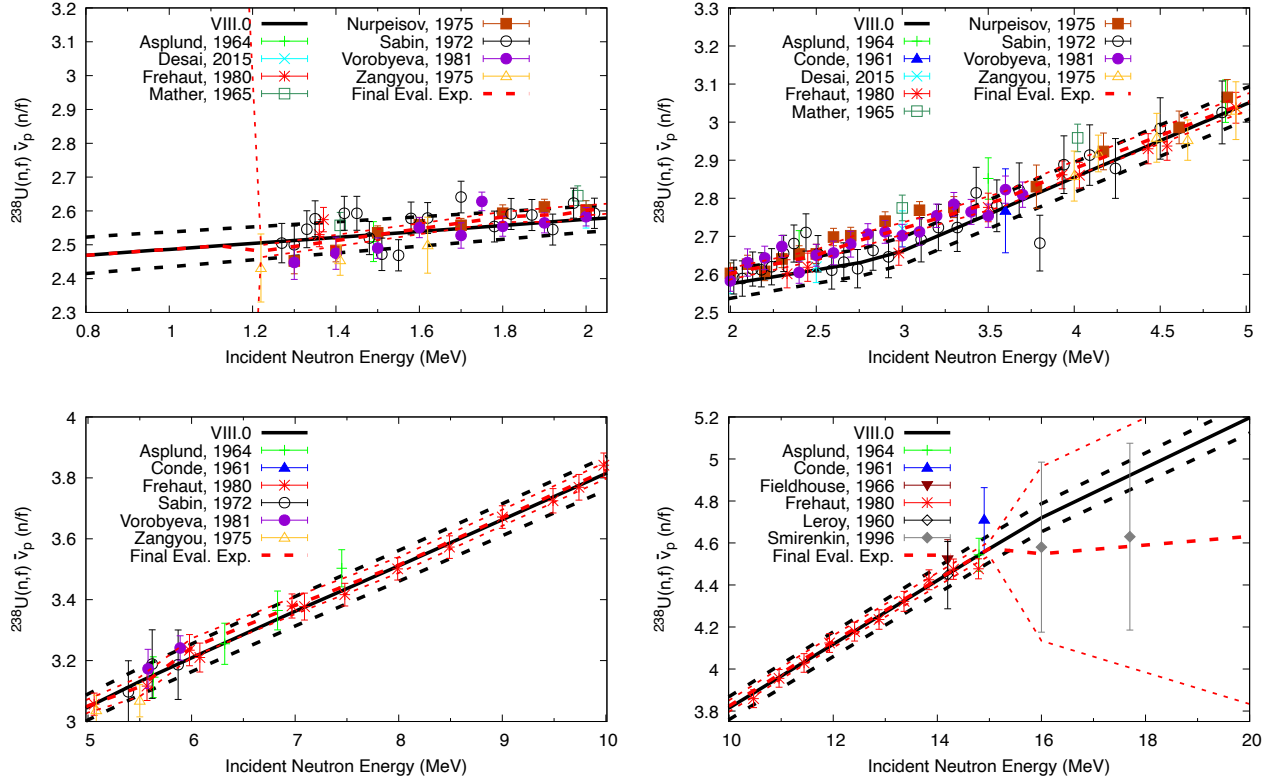


Figure 1: Evaluated $^{238}\text{U}(\text{n,f}) \bar{\nu}_p$ are shown in comparison to ENDF/B-VIII.0, and experimental data that were used for the evaluation. The evaluated data were obtained with a statistical analysis of only experimental data.

134 Iterative generalized least squares is usually executed until the evaluated results change negligibly.
 135 Here, this limit is reached after less than 10 iterations.

136 3 Results

137 3.1 Evaluated Results of $^{238}\text{U}(\text{n,f}) \bar{\nu}_p$ Based on Only Experimental Data

138 The evaluated results obtained from only experimental data via GLS in Fig. 1 differ from ENDF/B-
 139 VIII.0 from 2 to 4.5 MeV, from 6 to 7 MeV and above 15 MeV.

140 This difference from 2 to 4.5 MeV is caused by the fact that experts decided according to private
 141 communication with Roberto Capote (June 2, 2022) for ENDF/B-VIII.0 to follow the data of Fre-
 142 haut [9] in this energy range which is discrepant from the data of Nurpeisov [12] and Vorobyeva [14].
 143 The current evaluation is based on the generalized least technique described in Section 2.3 applied to
 144 all data deemed realistic, including Frehaut [9], Nurpeisov [12] and Vorobyeva [14]. The data of Sabin
 145 (sometimes also transliterated as Savin) [13] covers a similar energy range. It has scatter in the data
 146 and overlaps with all three data sets. These experiments face the challenge that ^{238}U has a significant
 147 angular distortion of fission fragments and prompt fission neutrons. Correcting for this effect is non-
 148 trivial, and can lead to bias in experimental $\bar{\nu}_p$. Hence, we cannot tell which of the four experiments
 149 is more accurate, and, consequently, whether the new evaluation or ENDF/B-VIII.0 is more realistic.
 150 Another differential experiment might be helpful. In fact, CEA will measure at LANSCE $^{238}\text{U} \bar{\nu}_p$
 151 with high precision and expect to deliver these experimental data in two years. Also validation with
 152 respect to post-scission fission observables via CGMF or with respect to effective neutron multiplication

153 factors, k_{eff} , of ICSBEP critical assemblies [25]. However, validation with respect to k_{eff} only makes
154 sense once we also include the new PFNS evaluation based on Chi-Nu and CEA experimental data to
155 counter-check the ENDF/B-VIII.0 PFNS.

156 The difference from 6 to 7 MeV could be caused by the fact that ENDF/B-VIII.0 smoothed over
157 second-chance fission structures visible in the experimental data. Such structures are expected from
158 physics point of view and as will be seen below are predicted by CGMF in a similar energy range.

159 Above 15 MeV, the evaluation follows Smirenkin data [24] that are systematically lower than
160 ENDF/B-VIII.0. These data were extracted from a PFNS measurement with low neutron-detection
161 efficiency, and impactful systematic corrections, such as multiple scattering, missing. Given these
162 flags raised and the significant lowering of the evaluated $\bar{\nu}_p$, it was decided to reject these data for
163 the evaluation including CGMF and instead using ENDF/B-VIII.0 values as pseudo-experimental data
164 starting from 15 MeV.

165 3.2 Evaluated Results of $^{238}\text{U}(\text{n},\text{f})$ $\bar{\nu}_p$ Including CGMF

166 The evaluated $^{238}\text{U}(\text{n},\text{f})$ $\bar{\nu}_p$ results are shown in Fig. 2. They are based on model-predicted values by
167 CGMF using evaluated parameter obtained by a Kalman fit to the experimental data listed in Tables I
168 and III. Several parameterizations were tested out. Here, we show three of them: (1) TKE is simulated
169 with a bend in first-chance fission and default fission probabilities in CGMF, (2) TKE is simulated with
170 a bend in first-chance fission and fission probabilities updated as shown in Fig. 3 and (3) TKE is
171 simulated without a bend in first-chance fission and with updated fission probabilities. The evaluated
172 data with CGMF are close to the evaluation based on only experimental data, with the evaluation using
173 TKE with a bend in first-chance fission and updated fission probabilities being closest to the evaluation
174 based on only experimental data. The evaluation without a bend in TKE is getting closer to the one
175 based on only experimental data from 1.6 until 2.25 MeV and from 11 to 15 MeV, but is significantly
176 higher than all other evaluations from 2.25 to 4.5 MeV. The second-chance fission threshold $\bar{\nu}_p$ with
177 CGMF is higher than without for all the three parameterizations used. This could be caused by a too
178 large second-chance fission probability at this energy.

179 Therefore, two parameterizations of the fission probabilities were explored. The default parameterization
180 in CGMF has a steep increase of second-chance fission from 5 to 6 MeV in the left-hand
181 side of Fig. 3 that in turn leads to a larger than realistic structure in the ^{238}U fission cross section
182 at second-chance fission. However, using the default versus the updated parameterization changes the
183 evaluated $\bar{\nu}_p$ only a little from 6 to 7 MeV in Fig. 2. The evaluated $\bar{\nu}_p$ using CGMF is above the experimental
184 $1-\sigma$ uncertainties of two Frehaut data points and one data point by Asplund. It is difficult to
185 get experimental data at second-chance fission as assumptions have to be made on the shape of the
186 PFNS of ^{252}Cf and ^{238}U . Usually, one and the same shape is assumed for those two PFNS across all
187 incident-neutron energies, which could lead to bias in experimental data at the second-chance fission
188 threshold where the ^{238}U PFNS is very different from the $^{252}\text{Cf}(\text{sf})$ PFNS. Also, again, the significant
189 angular distortion of fission fragment and prompt fission neutron emission of ^{238}U renders an analysis
190 of ^{238}U $\bar{\nu}_p$ difficult. Hence, CGMF results could indeed be realistic but this is difficult to know until
191 we get ^{238}U $\bar{\nu}_p$ data in two years. Further studies will be undertaken to see if the structure predicted
192 by CGMF at second-chance fission can be softened, and then a decision will have to be taken as to the
193 shape chosen for evaluated results.

194 3.3 Validation of Evaluated Parameters Against Various Fission Data

195 With the parameters from the evaluation with CGMF, we can calculate other prompt fission observables.
196 That enables studying how these observables, that were not included in the optimization, compare to
197 available experimental data. First, in Fig. 4, we show the pre-neutron emission mass distributions,
198 $Y(A)$, comparison among the two CGMF calculations with and without the TKE bend and available
199 experimental data. There are small differences between the two CGMF parametrizations in the peaks

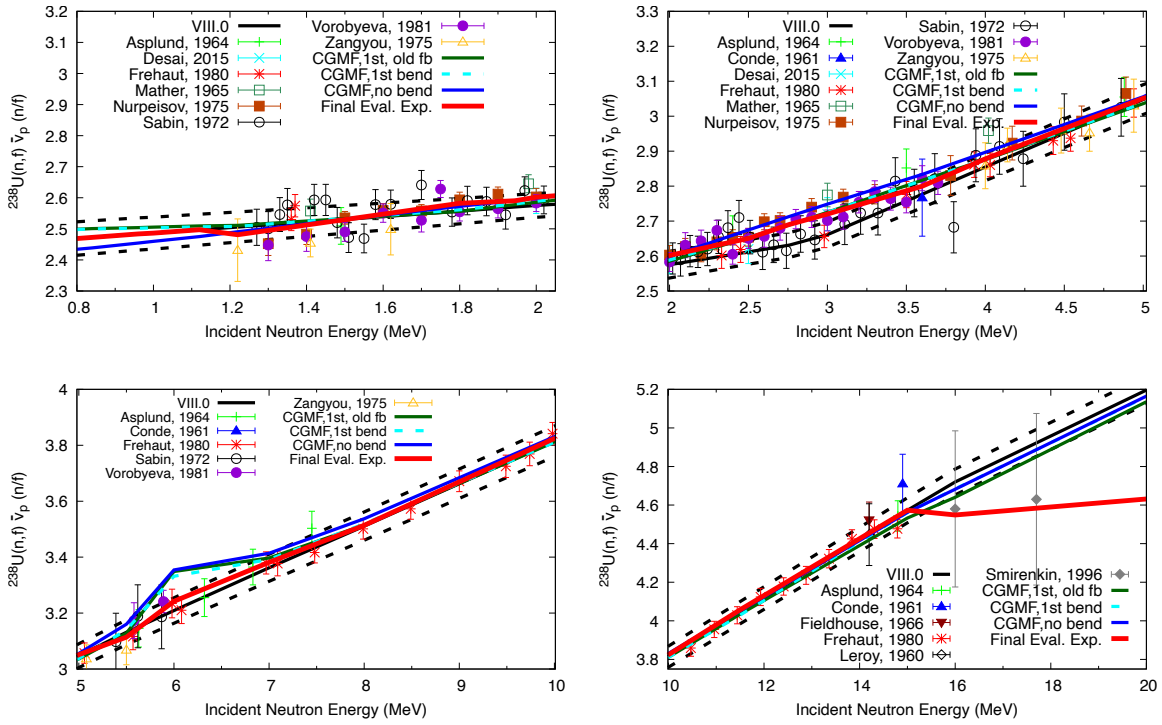


Figure 2: Evaluated $^{238}\text{U}(n,f)$ $\bar{\nu}_p$ are shown in comparison to ENDF/B-VIII.0 and experimental data that were used for the evaluation. The evaluated data were obtained with CGMF (with a bend in TKE for first-chance fission and without any bends in TKE, also results are included for the previous and new fission probabilities), and only experimental data.

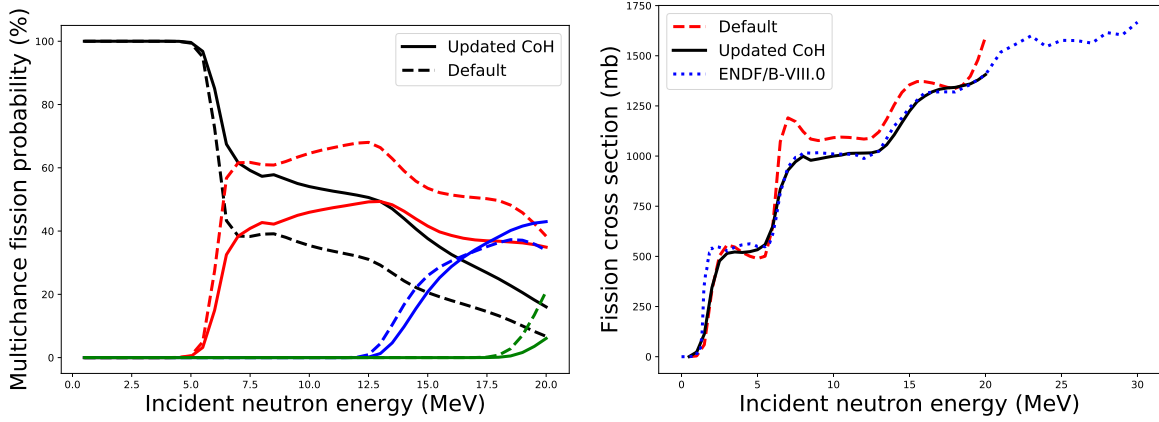


Figure 3: (Left-hand side) The default CGMF multi-chance fission probabilities for ^{238}U are compared to the updated ones. (Right-hand side) The $^{238}\text{U}(n,f)$ cross section related to these two parameterizations is shown and compared to ENDF/B-VIII.0 cross sections.

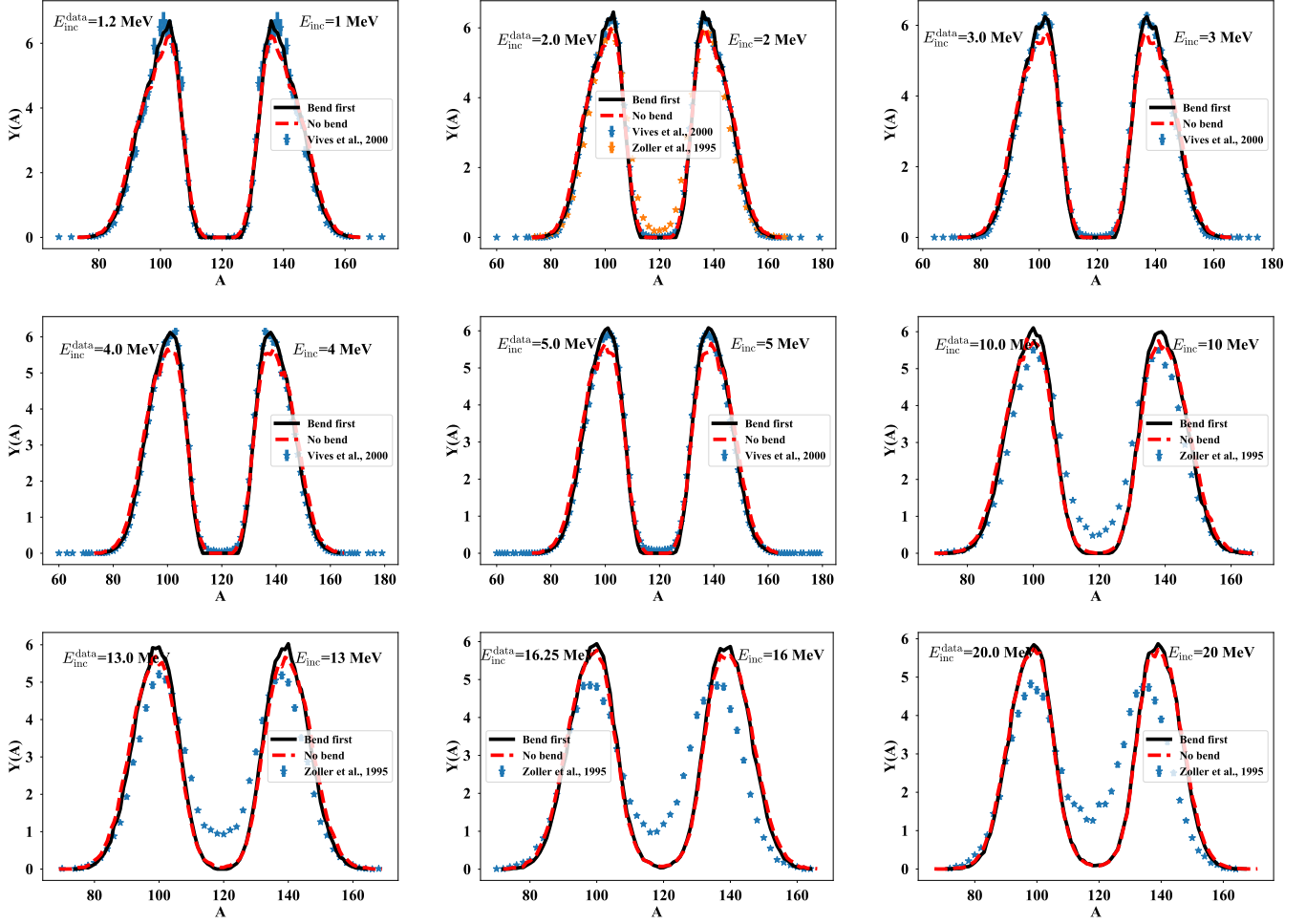


Figure 4: Comparison between CGMF results for $Y(A)$ calculated with parameters obtained by fitting $\bar{\nu}_p$ with and without the bend in the first-chance parametrization of the total kinetic energy. The incident energy of the experimental data is given in the upper left-hand side of each panel, while the incident energy of the CGMF calculation is given in the upper right-hand side.

200 of the distributions. The fit with a bend in TKE for first-chance fission better reproduces the mean
 201 of most of the data below the opening of second-chance fission; however, it is important to remember
 202 that these data are extracted from measurements after prompt neutron emission and the uncertainties
 203 are often under-reported. Above the second-chance threshold, the two CGMF parametrizations are
 204 essentially equally discrepant compared to the data.

205 Figure 5 provides the average total kinetic energy of the fission fragments as a function of incident
 206 neutron energy. The parametrization without the bend in the first-chance TKE reproduces TKE
 207 experimental data reasonably well, except at the lowest incident neutron energies (below about 3
 208 MeV). For the parametrization with a slope change, the change in slope is more curved than the
 209 default CGMF (the positive and negative slopes are less pronounced) and the calculated TKE is above
 210 most of the experimental data. Again, the data has to be extracted from measurements after neutron
 211 emission so there is often an $\sim 1\%$ uncertainty on the experimental values, even if it is not shown.
 212 In Fig. 6, we show $\overline{\text{TKE}}(A)$ and $\sigma_{\text{TKE}}(A)$ as a function of incident neutron energy. There are only
 213 large differences in the highest mass regions—towards $A = 160$. For $\sigma_{\text{TKE}}(A)$, the parametrization
 214 without the bend increases sharply at high masses, in an unphysical manner. Because of the high
 215 order polynomial, small changes in the parameters can lead to large changes in this observable that are

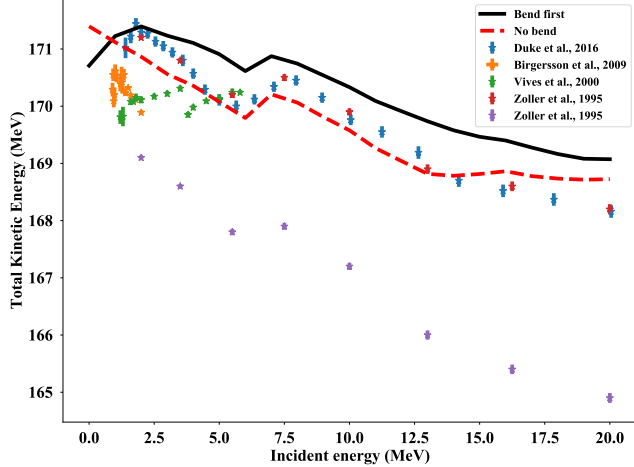


Figure 5: Total kinetic energy of the fission fragments as a function of incident neutron energy of the two CGMF parametrizations (with a bend in the first-chance parametrization and without a bend) and experimental data.

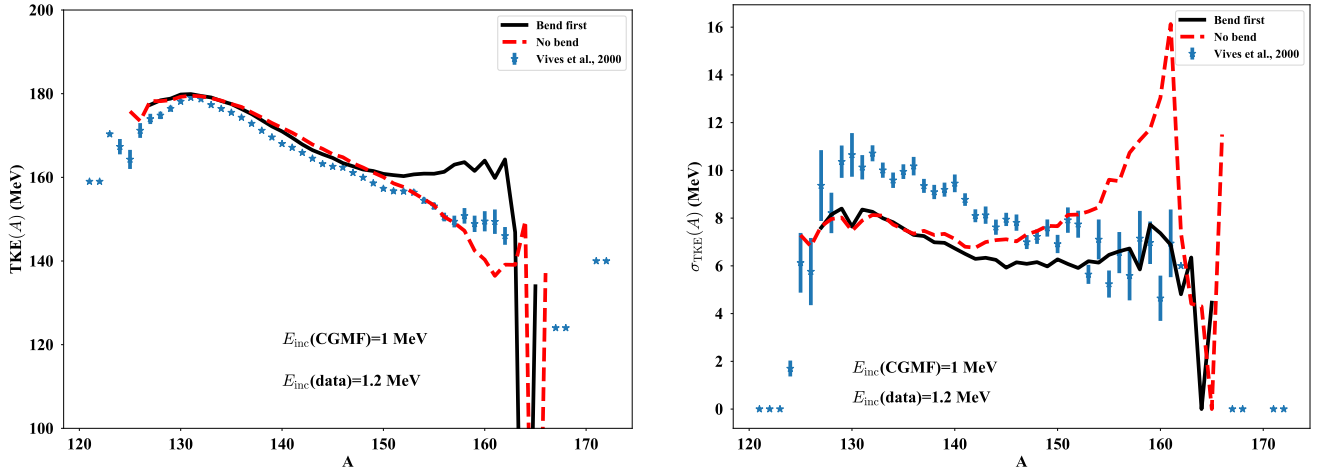


Figure 6: (Left) Total kinetic energy as a function of mass for 1 MeV incident neutrons. (Right) The width of the TKE distribution as a function of mass for 1 MeV incident neutrons.

not constrained by $\bar{\nu}_p$. Once again, these changes indicate that we should revisit this parametrization in CGMF, but cannot, unfortunately solve the question whether ENDF/B-VIII.0 or the new evaluation are more realistic from 2–4.5 MeV.

We then plot prompt neutron and γ -ray observables compared to available experimental data. First, in Fig. 7, we show the average prompt neutron energy for the two CGMF parametrizations. The largest difference between the two parametrizations is around $E_{\text{inc}} = 2.5$ MeV, the same incident energy where we see differences in the shape of the TKE. As in our previous reports, the average neutron energy from CGMF is systematically low compared to data—although from the limited data here, we reproduce the point at $E_{\text{inc}} = 15$ MeV very well. Additionally, as mentioned previously, Chi-Nu has measured the PFNS for $^{238}\text{U}(\text{n},\text{f})$, and it will be interesting to add this more complete data set to Fig. 7, in particular, to understand whether the striking feature at the opening of second-chance fission is accurate.

Figure 8 shows the average γ -ray multiplicity (left) and average γ -ray energies (right) as a function of incident neutron energy. There is almost no difference between the two CGMF parametrizations for

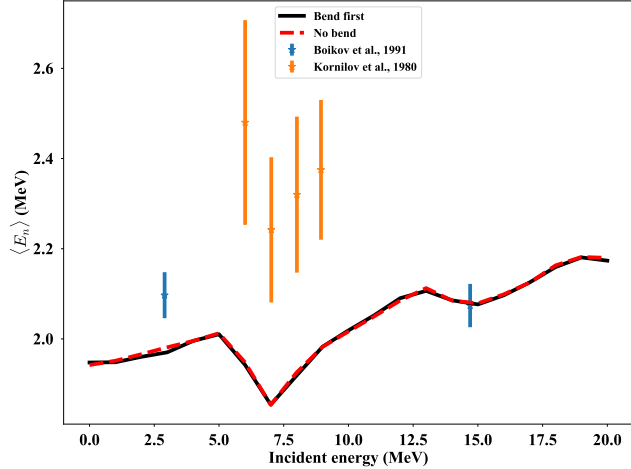


Figure 7: Average outgoing neutron energy from the two CGMF parametrizations compare to available experimental data.

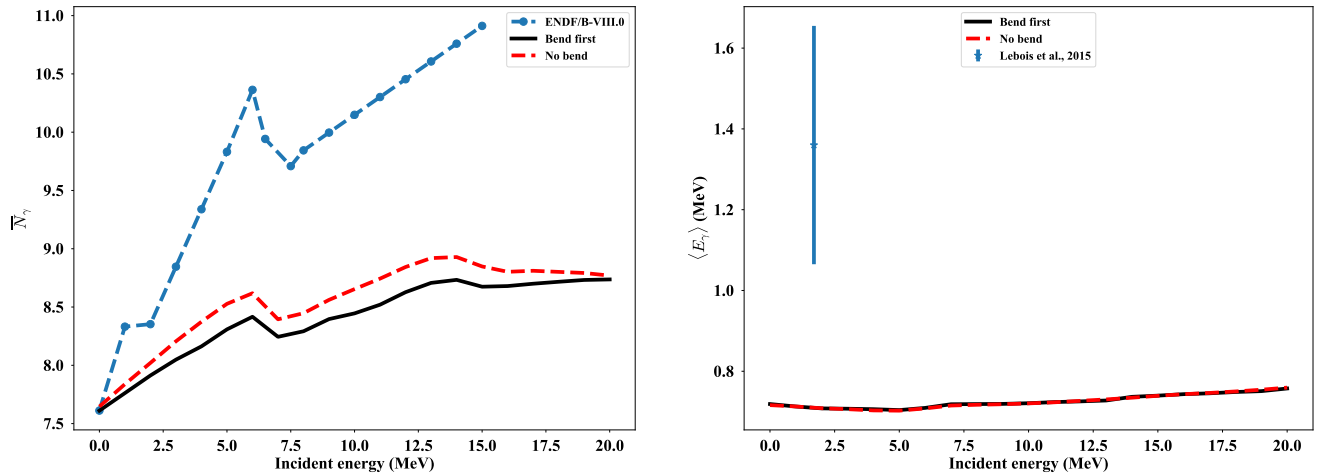


Figure 8: (Left) Prompt average γ -ray multiplicity from the two CGMF parametrizations compared to that of ENDF/B-VIII.0. (Right) Average prompt γ -ray energy from CGMF compared to one available data point.

230 the γ -ray energies, and only slight slope changes for the γ -ray multiplicities. These slope changes,
 231 again, come from the differences in the slope of the spin cutoff factor, α , but as of yet, cannot be
 232 directly compared to experimental data.

233 Finally, in Fig. 9, we show the neutron and γ -ray multiplicity distributions for the two parametriza-
 234 tions at an incident neutron energy of 1 MeV. The neutrons show some differences, particularly at $\nu = 0$
 235 and $\nu = 3$. The γ -ray multiplicity distributions, however, are essentially overlapping. From the prompt
 236 observables besides $\bar{\nu}_p$, there is little preference between the two CGMF parametrizations, besides in the
 237 sensitivity to the parameters in $\sigma_{\text{TKE}}(A)$, which has been discussed several times and requires further
 238 study.

239 4 Conclusions and Outlook

240 This report documents that we successfully completed an NCSP (Nuclear Criticality Safety Program)
 241 FY2022 Q4 milestone: “ ^{238}U : Evaluate PFNS and multiplicity consistently, including angular infor-

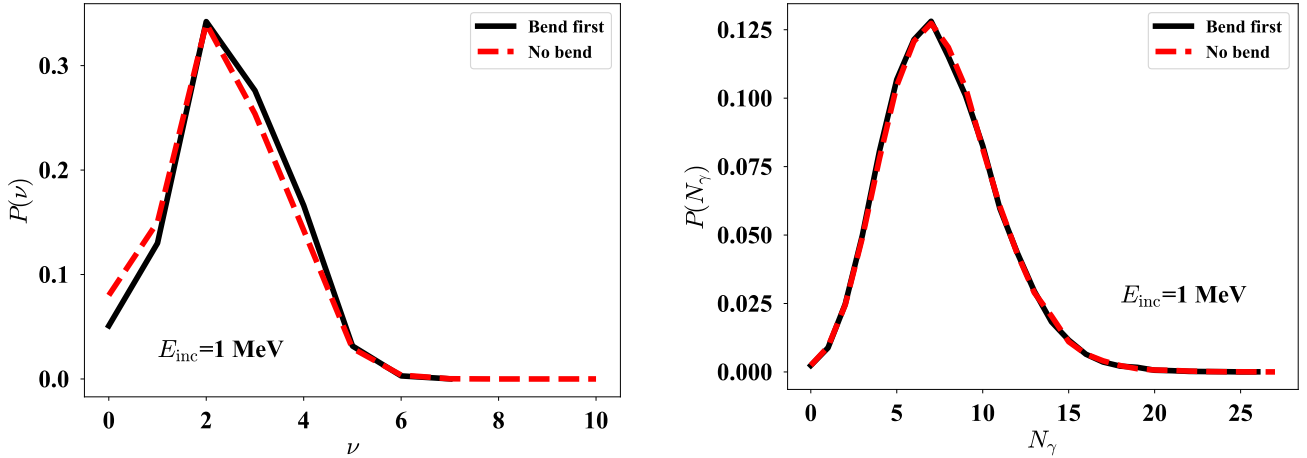


Figure 9: (Left) Neutron and (right) γ -ray multiplicity distributions from the two CGMF parametrizations at 1 MeV incident neutron energy.

mation about prompt neutrons". More specifically, we show that we evaluated $^{238}\text{U}(\text{n,f}) \bar{\nu}_p$ (termed "multiplicity" in the milestone text) with the code CGMF [1] that concurrently provides $\bar{\nu}_p$, angular information and prompt fission neutron spectra (PFNS).

This new evaluation of the $^{238}\text{U} \bar{\nu}_p$ had to be re-done from scratch as we did not have access to the input for the ENDF/B-VIII.0 evaluation. Thus, all experimental data were re-analyzed and their uncertainties estimated; several CGMF priors were established (using different parameterizations for $\langle TKE \rangle$, fission barrieris, etc.) and tested in evaluations and via comparison to fission observables. Here, we present two types of evaluations, one based on only experimental data differential experimental data, while the other also includes CGMF. The results from both evaluation types differ distinctly from ENDF/B-VIII.0 from 2 to 4.5 MeV, and from 6 to 7 MeV. The latter are structures commensurate with second chance fission and are expected from physics point of view. ENDF/B-VIII.0 $\bar{\nu}_p$ was likely smoothed and structures due to second-chance fission were removed by this smoothing of the data. Of larger concern is the distinct increase from 2 to 4.5 MeV. This is caused by ENDF/B-VIII.0 basing their data on Frehaut $\bar{\nu}_p$ that are systematically lower than the data of Nurpeisov and Vorobyeva from 2–4.5 MeV, and show a stronger inflection. For the analysis here, all three and additional data sets were taken into account leading to the distinctly larger (up to 2%) $\bar{\nu}_p$. Given the spread in data and the overall quality that can be gleaned from the journal articles of these data, it is not clear which experimental data are accurate and which ones are biased. Due to that, either ENDF/B-VIII.0 or the new evaluation can be correct.

Including modeling of CGMF does not change the evaluated data based on only experimental data, but follows it closely except for second chance fission which we are currently working on. This lends trust into that CGMF is able to produce evaluation-quality $\bar{\nu}_p$ as already has been seen for ^{239}Pu and $^{235}\text{U} \bar{\nu}_p$. If one forward-propagates evaluated parameters fitted to $^{238}\text{U} \bar{\nu}_p$ to various post-scission fission observables via CGMF, these predicted fission data correspond to experimental data except for TKE related observables. This could either hint towards a need to update some approximate CGMF parameterizations, or might point to issues in the new evaluated $\bar{\nu}_p$ from 2–4.5 MeV. A high-precision $^{238}\text{U} \bar{\nu}_p$ experiment from CEA, that will be possibly delivered in the next two years, might yield essential input here.

However, such big changes in $\bar{\nu}_p$ from ENDF/B-VIII.0 will have implications when simulating the effective neutron multiplication factor, k_{eff} , of ICSBEP critical assemblies [25] sensitive to ^{238}U from 2–4.5 MeV. One needs to counter-balance this change in k_{eff} due to an updated $\bar{\nu}_p$ to retain overall good performance in simulating critical assemblies.

274 In the near future, Chi-Nu PFNS experimental data are expected to be released. CEA PFNS
275 will likely delivered a year later. These will likely yield important input on the ^{238}U PFNS for which
276 only few independent measurements exist to date. It is possible that a new PFNS evaluation would
277 counter-balance the change coming from $\bar{\nu}_p$. Hence, the decision was taken to validate ^{238}U $\bar{\nu}_p$ once
278 the new PFNS is evaluated with Chi-Nu data, and then perform necessary tweaks. The evaluated
279 data will only be submitted together to a release candidate of a U.S. library to minimize the need for
280 tweaking given two changing observables. If, however, integral information paired with the new PFNS
281 yields no conclusive input on the deviation of the new evaluation from ENDF/B-VIII.0 from 2–4.5
282 MeV, we recommend holding off including the new $\bar{\nu}_p$ until the future CEA $\bar{\nu}_p$ experiment will provide
283 the necessary confirmation.

284 5 Point of contact

285 Denise Neudecker is the point of contact for questions on experimental data, the evaluation, and
286 validation with respect to various integral quantities. Amy E. Lovell is the point of contact for questions
287 on model calculations, model sensitivities, and validation with respect to various differential fission
288 data. Toshihiko Kawano helped in parameterizing second and third chance fission. Patrick Talou is a
289 CGMF expert and advised both Amy and Denise strongly on their work.

290 Acknowledgments

291 DN acknowledges insightful discussion with J. Taieb and B. Mauss (CEA) on their upcoming and
292 challenges in past $\bar{\nu}_p$ experiments. AEL would like to acknowledge useful discussions with I. Stetcu,
293 T. Kawano, and M. Herman. Work at LANL was carried out under the auspices of the National
294 Nuclear Security Administration (NNSA) of the U.S. Department of Energy (DOE) under contract
295 89233218CNA000001. We gratefully acknowledge partial support of the Advanced Simulation and
296 Computing program at LANL and the DOE Nuclear Criticality Safety Program, funded and managed
297 by NNSA for the DOE.

298 References

- 299 [1] P. Talou, T. Kawano, I. Stetcu et al. , “Fission Fragment Decay Simulations with the CGMF
300 Code,” *COMP. PHYS. COMM.* **269**, 108087 (2021).
- 301 [2] D. Neudecker, A.E. Lovell and P. Talou, “Producing ENDF/B-quality Evaluations of $^{239}\text{Pu}(n,f)$ and
302 $^{235}\text{U}(n,f)$ Average Prompt Neutron Multiplicities using the CGMF Model,” Los Alamos National
303 Laboratory Report **LA-UR-21-29906** (2021).
- 304 [3] A.E. Lovell, D. Neudecker and P. Talou, “Release of Evaluated $^{235}\text{U}(n,f)$ Average Prompt Fission
305 Neutron Multiplicities Including the CGMF Model,” Los Alamos National Laboratory Report **LA-UR-22-23475** (2022).
- 307 [4] A.E. Lovell, D. Neudecker, P. Talou, et al. , “Consistent Evaluation of the Prompt-Fission Neutron
308 Spectrum and Multiplicity for $n+^{235,238}\text{U}$ and $n+^{239}\text{Pu}$,” Los Alamos National Laboratory Report
309 **LA-UR-20-26932** (2020).
- 310 [5] I. Asplund-Nilsson, H. Conde and N. Starfelt, “Nu-bar of ^{238}U from 1.5 to 15 MeV,” *NUCLEAR
311 SCIENCE AND ENGINEERING* **20**, 527 (1964).
- 312 [6] H. Conde and N. Starfelt, “Measurement of nu in fast neutron fission of ^{232}Th and ^{238}U ” *NUCLEAR
313 SCIENCE AND ENGINEERING* **11**, 397 (1961).

314 [7] V.V. Desai, B.K. Nayak, A. Saxena et al. , “Prompt fission neutron spectra in fast-neutron-induced
 315 fission of ^{238}U ,” PHYSICAL REVIEW C **92**, 014609 (2015).

316 [8] D.S. Mather, M.H. McTaggart, A. Moat, “Revision of the Harwell ^{240}Pu source strength and nu for
 317 ^{235}U and ^{252}Cf ,” J.NUCLEAR ENERGY A&B **20**, 549 (1966).

318 [9] M. Soleihac, J. Frehaut and J. Gauriau, “Energy Dependence of $\bar{\nu}_p$ for Neutron-induced Fission of
 319 ^{235}U , ^{238}U and ^{239}Pu from 1.3 to 15 MeV,” J. OF NUCL. ENERGY **23**, 257–282 (1969); J. Frehaut,
 320 G. Mosinski and M. Soleihac, “Recent Results in $\bar{\nu}_p$ Measurements between 1.5 and 15 MeV,” Top-
 321 ical Conference on $\bar{\nu}_p$ The Average Number of Neutrons Emitted in Fission, France, 1972, Report
 322 EANDC(E)-15 “U” (1973).

323 [10] J. Leroy, “Mean number of prompt neutrons emitted in the fission of ^{238}U , ^{239}Pu , ^{232}Th ,” JOURNAL
 324 DE PHYSIQUE **21**, 617 (1960).

325 [11] D.S. Mather, P. Fieldhouse and A. Moat, “Measurement Of Prompt $\bar{\nu}$ For The Neutron-Induced
 326 Fission Of Th^{232} , U^{233} , U^{234} And Pu^{239} ,” NUCLEAR PHYSICS **66**, 149 (1965).

327 [12] B. Nurpeisov, K.E. Volodin, V.G. Nesterov et al. , “Dependence of $\bar{\nu}$ on neutron energies up to
 328 5. MeV for ^{233}U , ^{238}U and ^{239}Pu ,” SOVIET ATOMIC ENERGY **39**, 807 (1975).

329 [13] M.V. Sabin, Yu.A. Khokhlov, I.N. Paramonova et al. , “Energy dependence of average neutron
 330 number for fast-neutron fission of ^{238}U ,” SOVIET ATOMIC ENERGY **32**, 474 (1972).

331 [14] V.G. Vorobyeva, B.D. Kuzminov, V.V. Malinovskij et al. , “Analysis of the energy dependence
 332 of the average number of prompt neutrons for neutron-induced fission of ^{238}U ,” VOP. AT.NAUKI I
 333 TEKHN. **1/40**, 62 (1981).

334 [15] B. Zongyu, “The variation of average prompt neutron number for ^{238}U fission in the fast neutron
 335 energy region with incident neutron energy,” ATOMIC ENERGY SCIENCE AND TECHNOLOGY **9**,
 336 362 (1975).

337 [16] D. Neudecker, “ARIADNE—a program estimating covariances in detail for neutron experi-
 338 ments,” EPJ-N **4**, 34 (2018).

339 [17] D. Neudecker, A. Lewis, E. Matthews et al., “Templates of Expected Measurement Uncertain-
 340 ties,” Los Alamos National Laboratory Report LA-UR-19-31156 (2019).

341 [18] A.D. Carlson et al. , “Evaluation of the Neutron Data Standards,” NUCL. DATA SHEETS **148**,
 342 143 (2018).

343 [19] D.A. Brown, M.B. Chadwick, R. Capote et al. , “ENDF/B-VIII.0: The 8th Major Release of the
 344 Nuclear Reaction Data Library with CIELO-project Cross Sections, New Standards and Thermal
 345 Scattering Data,” NUCL. DATA SHEETS **148**, 1–142 (2018).

346 [20] D. Neudecker, P. Talou, T. Kawano et al. , “Evaluations of Energy Spectra of Neutrons Emitted
 347 Promptly in Neutron-induced Fission of ^{235}U and ^{239}Pu ,” NUCL. DATA SHEETS **148**, 293 (2018).

348 [21] D. Neudecker, R. Frühwirth and H. Leeb, “Peelle’s Pertinent Puzzle: A Fake due to Improper
 349 Analysis,” NUC. SCI. ENG. **170**, 54–60 (2012).

350 [22] R. Peelle, “Peelle’s pertinent puzzle,” Informal Oak Ridge National Laboratory Memorandum
 351 (1987).

352 [23] S. Chiba, D. L. Smith, "A suggested procedure for resolving an anomaly in least-squares data
 353 analysis known as "peelle's pertinent puzzle" and the general implications for nuclear data eval-
 354 uation," JOURNAL OF NUCLEAR SCIENCE AND TECHNOLOGY **148**, 1–30 (1991).

355 [24] G.N. Smirenkin, G.N. Lovchikova, A.M. Trufanov *et al.*, "Measurement of energy spectrum of
 356 neutrons accompanying emission fission of U-238 nuclei," YADERNAYA FIZIKA, **59**, 1934 (1996).

357 [25] J. Bess (editor), "International Handbook of Evaluated Criticality Safety Benchmark Experiments
 358 (ICSBEP)," Organization for Economic Co-operation and Development-Nuclear Energy Agency
 359 Report NEA/NSC/DOC(95)03 (2019).

360 **A Comments on Experimental Data for ^{238}U $\bar{\nu}_p$**

361 **Asplund 1964** They measured with two different mono-energetic neutron sources but also per-
 362 formed TOF for energy determination at higher incident-neutron energy to distinguish spurious neu-
 363 tron groups. They used the ratio liquid-scintillator technique. A coincidence between FF and PF
 364 gammas in scintillator (doped with Gd) was used as a start of the gate. Most uncertainties are take
 365 from the template as the authors generally gave correction factors rather than uncertainties. The
 366 template values are within a credible range given the corrections that the authors mention. All in all,
 367 a well-done data set that is described in detail. It seems that Asplund 1964 and Conde 1961 are corre-
 368 lated. They share 2 common authors and the description of the detector is very similar. Asplund was
 369 aware of many necessary corrections, but delayed gammas, displacement of samples, sample impurity
 370 and forward boost were not corrected for. The data seems systematically higher than evaluation > 2
 371 MeV. The gate is open for a reasonably long time (45 μs).

372 **Conde 1961** They measured with one mono-energetic neutron source but also performed TOF for
 373 energy determination at higher incident energy to distinguish spurious neutron groups. They used
 374 the ratio liquid-scintillator technique. A coincidence between FF and PF gammas in scintillator (doped
 375 with Gd) was used as a start of the gate. Most uncertainties are take from the template as the authors
 376 generally gave correction factors rather than unc. The template values are within a credible range
 377 given the corrections that the authors mention. All in all, a well-done data set that is described in
 378 detail. It seems that Asplund 1964 and Conde 1961 are correlated. They share 2 common authors
 379 and the description of the detector is very similar. This is a well-documented data sets. Conde was
 380 aware of many necessary corrections, but delayed gammas, displacement of samples, sample impurity,
 381 sample thickness and forward boost were not corrected for. The data seems systematically higher than
 382 evaluation at 14 MeV. The gate is open for a short time (30 μs).

383 **Desai 2015** his is an unusual measurement. It is a PFNS measurement, from which they extracted
 384 $\bar{\nu}_p$. The experimental data agree well. I am worried about their missing multiple-scattering correction
 385 as this can cause a sizable contribution on a PFNS measurement. However, they took the ratio to
 386 ^{252}Cf . The correction in their PFNS can amount to 2%. I add a 1.0% multiple scattering uncertainty
 387 for $\bar{\nu}_p$. Also, they did not correct for angular distribution, something that is very important for ^{238}U
 388 and when measuring with two neutron detectors. Therefore, adding unc. The paper does not state
 389 how they got multiplicities. I assume extrapolation and would add 0.5% for that given that the PFNS
 390 starts at 0.7 MeV. The "total" uncertainties are low, so I assume them to be statical in nature and add
 391 templates on top. Missing corrections: multiple scattering, angular distribution, sample thickness.

392 **Fieldhouse 1966** The level of documentation and knowledge that went in this experiment of 1966
 393 is impressive. Fieldhouse and Moat provided also input data for the $^{252}\text{Cf}(\text{sf})$ standard and knew what
 394 they were doing. The 14-MeV point is very uncertain but agrees reasonably well with other exp. and

395 eval. data. They have a good neutron-detection efficiency (0.89% with 0.2% uncertainty.) The gate
396 was open reasonably long (40 μ s). They provided PFNS uncertainties, but I rather take my own. They
397 were aware of many corrections and did a great job. Did an estimate of delayed gammas but could
398 not calculate it. Not many uncertainties are given but templates fit together with reported sizes of
399 corrections.

400 **Frehaut 1980** This is a well-documented data sets. Frehaut was aware of many necessary corrections,
401 but one has to look a bit at later publications to figure out what corrections were applied to the data.
402 The data seems systematically lower than the evaluation but that might be caused by a bit too low a
403 monitor value that Frehaut used. The gate is open for a reasonably long time (50 μ s). Julien mentioned
404 there is an issue with the data because of (n,2n) and $\bar{\nu}_p$ competition not correctly resolved. Frehaut
405 cites a total systematic uncertainty of 0.5%.

406 **Leroy 1960** This is a well-documented data set and they were aware of many effects for the time
407 (1960). Unfortunately, the documentation is in French making an in-depth analysis somewhat hard.
408 The 14.2 MeV point agrees well with evaluated data and other exp. data. Gate time could not be
409 found. They give rather large detector efficiency (PFNS) uncertainties. They were aware of many
410 corrections and did a great job. Missing corrections: delayed gammas, sample thickness, displacement
411 of sample.

412 **Mather 1965** This is a medium well-documented data sets. They were aware of many effects that
413 need to be corrected for. I am worried by the fact that they use Pt backing foils that are known to lead
414 to necessary Coulomb corrections for (n,f). Not sure if they studied it here. It reads like they are using
415 $^{252}\text{Cf(sf)}$ $\bar{\nu}_t$. They got the detector efficiency with that measurement. The data are systematically
416 high. Missing correction: delayed gammas, sample thickness and displacement of sample.

417 **Nurpeisov 1975** They did a very good job describing what was corrected. Their data agrees well
418 with the bulk of other experimental data except in the dip around 2.75 MeV. A 75% detector efficiency
419 is reasonable. The gate is open for a long time (100 μ s). However, this is explained by the time
420 the neutron spends inside the detector (50 μ s) on average and seems to be a material-dependent
421 quantity. They get the random coincidence (sometimes termed false-fission events) by measuring 250
422 ns after the fission pulse is detected. Sounds reasonable. Multiple scattering effects were reduced
423 by shielding. Detector efficiency was measured. Therefore, the usual PFNS uncertainty is replaced
424 by detector efficiency uncertainty. They had problems with beam stability above 3.5 MeV. Did a
425 good job at uncertainty quantification and corrections. Explicit uncertainties are given for correction
426 factors which will be used as uncertainties. Two effects they missed: delayed gammas and sample
427 displacement, so uncertainties from the template were taken. I also added impurity uncertainty as I
428 don't have much information to go by.

429 **Sabin 1972** The data have a wave-like structure that makes me wonder about their statistical
430 uncertainties. The TOF length is 35 m, with a time resolution of 1 ns/m that was used to calculate an
431 energy uncertainty. Fission was detected by prompt gammas. They accounted for multiple scattering
432 in the sample, sample holder/ backing (Pb) by doing measurements just with the sample holders/
433 backing. The neutron-detector efficiency assumes a value of 70%. That is not the best value but
434 reasonable. The statistical uncertainty of the combined data set is 0.8-1.8%. The neutron-detection
435 efficiency uncertainty is given with 0.5% which replaces the PFNS uncertainty. Background uncertainty
436 of 1.0% + 0.5% capture uncertainty is given. It seems that the total uncertainties in EXFOR consist
437 of neutron-detection efficiency uncertainties, background uncertainties, and statistical uncertainties.

438 Hence, the latter can be backed out. Multiple scattering corrections are given with 4-8%. I take 0.5%
439 as uncertainty.

440 **Vorobyeva 1981** The data were very well documented with regards to uncertainties and correction
441 factors. they thought of many pertinent corrections. The only missing correction was delayed gam-
442 mas. The data meander around VIII.0. Uncertainties for PFNS, sample displacement, many types of
443 background, sample thickness, energy, and of statistical nature were explicitly provided.

444 **Zangyou 1975** This data set is documented in a Chinese article, so I could not read it, but EX-
445 FOR gave the impression of a fairly detailed analysis. Many uncertainty sources or corrections were
446 discussed. The data seem systematically lower at low energies and too high at high energies. It is
447 unknow how long the gate was open.

448 **Rejected data sets because measured above 20 MeV** Frehaut (1980_2), EXFOR-number:
449 21685.003: Data are measured at energies larger than 20 MeV. We will only evaluate until 20 MeV
450 and then revert to ENDF/B-VIII.0. But this library seems to have take Frehaut (1980_2) anyway.

451 **Rejected data sets because either clearly outlying, or for physics reasons, too large uncer-
452 tainties or insufficient uncertainty information provided both in EXFOR or the literature**

- 453 • Barnard (1965): No uncertainties are reported but data fall right on VIII.0. The data were
454 extracted from a PFNS measurement. While the data were “measured” as part of experiment,
455 they seem to be derived from fitting PFNS data to a Maxwellian and then backing out the $\bar{\nu}_p$.
456 Given the lack of information and uncertainties, I reject those data.
- 457 • Baryba (1979): The data are 15% off at 14.7 MeV. Extracted from PFNS measurement, measured
458 at 1 angle (at 14.7 MeV this would lead to angular bias). I could not get any documentation
459 and many corrections are missing (only attenuation and background are mentioned, no angular
460 distribution, no energy extrapolation, etc.).
- 461 • Bethe (1955): The data are 5% off at 4.5 MeV. The uncertainties are in the range of 13%.
462 The information in EXFOR is extremely scarce. This measurement will have no impact on the
463 evaluation and is clearly biased.
- 464 • Boikov (1991): This is an unusual measurement. It is a PFNS measurement, from which they
465 extracted $\bar{\nu}_p$. The experimental data are too low at 14 MeV and are too high at 2.9 MeV. Angular
466 distributions are not considered and can bias ^{238}U more than ^{239}Pu and ^{235}U .
- 467 • Butler (1962): Unfortunately, the data are very scarcely described in EXFOR (no information
468 on set-up, unc., etc.), and the journal publication cannot be retrieved. It is only one data point.
- 469 • Bondarenko (1958): The data are 11% off at 4.0 MeV. The uncertainties are in the range of 3%.
470 The information in EXFOR is extremely scarce and the proceeding can only be bought. This
471 measurement will have no impact on the evaluation and is clearly biased.
- 472 • Diven (1957): This data set is vvery scarcely described. Not even the monitor is given and
473 in Diven’s case this could be both ^{235}U -235 $\bar{\nu}$ at thermal or $^{252}\text{Cf(sf)}$ $\bar{\nu}$. The publication is a
474 theoretical paper with no experimental details, the EXFOR entry is very short. Also, the data are
475 systematically high (6%) which could be due to an outdated monitor. It is also fairly uncertain
476 (3.4%).

477 • Flerov (1958): This is an unusual experiment. They measure the total production of neutrons for
 478 14.1-MeV neutrons in then subtracted (n,2), (n,inl) and divide through the fission cross section.
 479 They did not have an (n,inl) cross section, so they extrapolated it. We do not know (today,
 480 not 1958) the cross section to better than 25%. It is amazing that the datapoint is only 3%
 481 lower than VIII.0. This data set is much too uncertain and riddled with too many systematic
 482 unknowns to be considered.

483 • Johnstone (1965): The gate was open too long (500 μ s), will measure a lot of background. The
 484 monitor is also not properly described in the EXFOR entry. This is natural uranium. The
 485 statistical uncertainty is large (4.5%). The data will likely have no impact at all and are rejected.
 486 Not surprisingly that data are outlying. Missing corrections: attenuation, sample thickness,
 487 angular distribution of FF (at 14 MeV), forward boost (at 14 MeV), geometry, displacement of
 488 sample. The data point at 2.5 MeV is too low by 10% and 7%, at 14 MeV.

489 • Kornilov (1980): The data are very outlying (10% low). The first article is in Russain. The
 490 second one presents data for another incident-neutron energy range by Zhurvalev in Table 2 and
 491 Table 3 Kornilov data. The latter, which are actually in EXFOR, are extracted from a PFNS. I
 492 might take Zhuarvlev data but not Kornilov data in EXFOR.

493 • Kuzminov (1961): The documentation of the data could not be obtained and they are scarcely
 494 described in EXFOR. They are also highly outlying (8%).

495 • Laurent (2014): The neutron detector efficiency is 30% for below 1 MeV and goes down to
 496 10% at 10 MeV. I.e., you need huge corrections. Given that, the results are surprisingly well in
 497 agreement with VIII.0. BUT, the statistical uncertainties are HUGE, on the order of 3% to 10%.
 498 For some data points, you really see the scatter and the data are highly outlying. I doubt if the
 499 data would have any impact at all. It should be mentioned that these were only auxiliary data
 500 used to test their detector. No systematic uncertainties are provided.

501 • Sher (1960): The data are 5% off from VIII.0 and have 12% unc. I.e., they will have little impact.
 502 They also use a reactor spectrum rather than an accelerator which makes one wonder about the
 503 incident energy they see.

504 • Smirenkin (1966): This measurement extracts $\bar{\nu}_p$ from a PFNS measurement. They take the
 505 $^{252}\text{Cf(sf)}$ PFNS as a reference, and then back the detector efficiency out. So, in a sense it is an
 506 absolute measurement. They excluded secondary neutrons via TOF. Background was reduced
 507 via TOF and shielding. Fission fragments were detected via a fission chamber coincident with
 508 neutron detectors. The time-of-flight length is 1.7 m with a time resolution of 2.5-3 ns. 30%
 509 detection efficiency for neutrons is very low. This is a matter of concern. No correction on
 510 multiple scattering is mentioned. That is a problem for a PFNS, especially, one that is so far
 511 from the reference of $^{252}\text{Cf(sf)}$ PFNS at this energy. Given this important missing correction, I
 512 leave the total unc. as statistitical. Missing corrections : impurity; deadtime; sample thickness;
 513 multiple scattering. As it is the only measurement above 15 MeV, I left it at first in despite the
 514 many flags raised. But the values were biased low and adversely impacted the evaluated ^{238}U
 515 $\bar{\nu}_p$. So, in the end, I rejected it after all.

516 • Taieb (2007): The data were obtained through a PFNS measurement using the FIGARO array.
 517 This is a predecessor of the Chi-Nu array. John O'Donnell from both the FIGARO and Chi-Nu
 518 teams had highlighted previously there that are systematic issues with that array (background),
 519 and that was why the array was replaced by Chi-Nu. Time resolution was also large, they
 520 covered only angles from 45 to 135 degree. Angular distributions matter especially or ^{238}U at
 521 low energies, where data are systematically over-predicted (7% high at 2.5 MeV) The spectrum

522 is measured from 0.7-7.0 MeV, otherwise, they extrapolated with a Watt spectrum. To make
523 matters worse, they calibrated their measurement to Boikov 2.9 MeV PFNS, which raised flags
524 as well. They did not measure pre-equilibrium because of the 7-MeV E_{out} cut-off and their $\bar{\nu}_p$
525 is systematically low above 10 MeV (7% high at 13 MeV). The data are rejected for the reasons
526 above. Also, the experimental uncertainties are scarce and the data set is preliminary.

- 527 • Vasilev (1960): I could not find the article (journal out of print) and the EXFOR entry is the
528 barest skeleton I have seen so far. I have no clue what was corrected for, if there was a monitor
529 used, what the uncertainties are. In addition to that, the data point is outlying (3%) and highly
530 uncertain (7%). I reject it given the lack of information.
- 531 • Voignier (1968): Very little information in EXFOR entry, no paper found and derived from elastic
532 and inelastic scattering with 9% detector efficiency uncertainty. This data set would have very
533 little impact and is not informed well enough for the evaluation.
- 534 • Yamamoto (1979): No uncertainty information and uncertainties given. Corrections are not well
535 described. $\bar{\nu}_p$ is derived from "Neutron emission, Mass distribution and Energetics", so not a
536 typical $\bar{\nu}_p$ measurement. $\bar{\nu}_p$ data are just a by-product of the measurement, not meant as a $\bar{\nu}_p$
537 experiment.